

## Synthesis of Aligned Arrays of Millimeter Long, Straight Single-Walled Carbon Nanotubes

Zhen Yu, Shengdong Li, and Peter J. Burke\*

*Integrated Nanosystems Research Facility,  
Department of Electrical Engineering and Computer  
Science, University of California, Irvine,  
Irvine, California 92697-2625*

*Received March 23, 2004*

*Revised Manuscript Received July 15, 2004*

The unique electrical and mechanical properties of single-walled carbon nanotubes (SWNTs) have motivated rapid progress in nanotube synthesis and electronics in the past few years.<sup>1</sup> Many significant initial steps have been taken. For example, simple circuits based on SWNTs have recently been demonstrated.<sup>2–4</sup> However, large-scale integration on a level comparable to current microelectronics, although in principle achievable, is still an elusive goal. In this work, we take a step closer to this goal by demonstrating the controlled growth of millimeter long, straight arrays of SWNTs in a single-furnace chemical vapor deposition (CVD) system.

Currently, three general methods exist for the synthesis of SWNTs:<sup>5</sup> Arc discharge, laser ablation, and CVD. CVD has the advantage that the catalyst structures that initiate growth can be defined lithographically, initially demonstrated by Kong et al.,<sup>6</sup> a significant first step toward large-scale integration of nanosystems. Kong et al. used methane as the feedstock and showed that high-quality SWNTs of length  $\sim 10 \mu\text{m}$  could be grown on Si wafers; the orientation of the nanotubes was not controlled.

Subsequent work by the same group showed that with use of a combination of methane, ethylene, and  $\text{H}_2$  as the feedstock, SWNTs up to  $600 \mu\text{m}$  in length could be synthesized. These were also randomly oriented and contained  $\sim 10$  loops along their length, i.e., were not straight but rather “curly”. Using the same growth recipe of methane, ethylene, and  $\text{H}_2$  feedstock CVD, the Fuhrer group recently synthesized and electrically contacted a single  $300 \mu\text{m}$  long, straight SWNT.<sup>7</sup> Other research has shown that when an electric field is applied during growth, SWNTs grown by CVD can be aligned

parallel to the direction of the electric field.<sup>8–10</sup> Recently, the Liu group has demonstrated outstanding results in the synthesis of arrays of long SWNTs.<sup>11–15</sup> They developed a technique based on “fast-heating”. Using this technique and  $\text{CO}/\text{H}_2$  as the feedstock, they demonstrated the growth of arrays of SWNTs  $\sim 1 \text{ mm}$  in length and observed SWNTs up to approximately  $1 \text{ cm}$  in length. They also demonstrated crossed arrays of SWNTs.

In this work, we demonstrate the growth of arrays of  $1.5 \text{ mm}$  long, straight single-walled nanotubes fabricated using a single furnace with methane and  $\text{H}_2$  as the feedstock. Our work shows that arrays of long, straight nanotubes can be grown in a single furnace system, without the need for rapid heating, thus simplifying the synthesis procedure.

For the pre-growth catalyst preparation, we started with a 4-in. Si wafer (100, p-type, resistivity  $12\text{--}16 \text{ k}\Omega\text{-cm}$ ) with a  $500 \text{ nm}$  thick  $\text{SiO}_2$  film as a substrate. A thin Cr/Au ( $50 \text{ nm}/200 \text{ nm}$ ) bilayer was deposited by e-beam or thermal evaporation and patterned photolithographically using liftoff. After definition of the metallization pattern, photoresist was applied, exposed, and developed, to fabricate wells in the resist over the Cr/Au pattern. An aqueous suspension of Fe-laden alumina nanoparticle catalysts was applied and allowed to dry in air and then lifted off in acetone. The result is a lithographically defined Cr/Au/nanoparticle catalyst pattern ready for growth. Since our catalyst suspension is aqueous based, it is compatible with standard photoresist and economical optical lithography, in contrast to the method of Kong, which uses a methanol-based suspension requiring PMMA, hence electron beam lithography or special deep UV lithography.

The nanoparticle suspension was prepared by adding  $0.3 \text{ g}$  of alumina nanoparticles (Degussa, aluminum oxide C),  $0.05 \text{ mmol}$  of  $\text{Fe}(\text{NO}_3)_3 \cdot 9\text{H}_2\text{O}$  (Aldrich), and  $0.015 \text{ mmol}$  of  $\text{MoO}_2(\text{acac})_2$  (Aldrich) to  $300 \text{ mL}$  of DI water ( $18 \text{ M}\Omega\text{-cm}$ ). The mixture was stirred for  $24 \text{ h}$  and sonicated for  $1 \text{ h}$ . In this work, different diluted nanoparticle catalyst solutions have been investigated for nanotube growth.

The synthesis was carried out using a home-built CVD system based on a 3 in. diameter Lindberg furnace, with a specially designed gas-flow injector to minimize turbulent flow. The growth procedure was as follows: First, the sample was heated to  $900 \text{ }^\circ\text{C}$  in Ar over the course of  $0.5 \text{ h}$ . Next,  $\text{H}_2$  was flowed for  $10 \text{ min}$ . Next, a

\* To whom correspondence should be addressed. E-mail: pburke@uci.edu.

(1) McEuen, P. L.; Fuhrer, M. S.; Park, H. K. *IEEE Trans. Nanotechnol.* **2002**, *1*, 78–85.

(2) Bachtold, A.; Hadley, P.; Nakanishi, T.; Dekker, C. *Science* **2001**, *294*, 1317–1320.

(3) Derycke, V.; Martel, R.; Appenzeller, J.; Avouris, P. *Nano Lett.* **2001**, *1*, 453–456.

(4) Javey, A.; Wang, Q.; Ural, A.; Li, Y. M.; Dai, H. J. *Nano Lett.* **2002**, *2*, 929–932.

(5) Dresselhaus, M. S., Dresselhaus, G., Avouris, P., Eds. *Carbon nanotubes: synthesis, structure, properties, and applications*; Springer: Berlin, 2001.

(6) Kong, J.; Soh, H. T.; Cassell, A. M.; Quate, C. F.; Dai, H. J. *Nature* **1998**, *395*, 878–881.

(7) Durkop, T.; Getty, S. A.; Cobas, E.; Fuhrer, M. S. *Nano Lett.* **2004**, *4*, 35–39.

(8) Zhang, Y. G.; Chang, A. L.; Cao, J.; Wang, Q.; Kim, W.; Li, Y. M.; Morris, N.; Yenilmez, E.; Kong, J.; Dai, H. J. *Appl. Phys. Lett.* **2001**, *79*, 3155–3157.

(9) Ural, A.; Li, Y. M.; Dai, H. J. *Appl. Phys. Lett.* **2002**, *81*, 3464–3466.

(10) Joselevich, E.; Lieber, C. M. *Nano Lett.* **2002**, *2*, 1137–1141.

(11) Huang, S. M.; Cai, X. Y.; Liu, J. *J. Am. Chem. Soc.* **2003**, *125*, 5636–5637.

(12) Huang, S. M.; Cai, X. Y.; Du, C. S.; Liu, J. *J. Phys. Chem. B* **2003**, *107*, 13251–13254.

(13) Huang, S. M.; Maynor, B.; Cai, X. Y.; Liu, J. *Adv. Mater.* **2003**, *15*, 1651–1655.

(14) Zheng, B.; Lu, C. G.; Gu, G.; Makarovski, A.; Finkelstein, G.; Liu, J. *Nano Lett.* **2002**, *2*, 895–898.

(15) Huang, S.; Woodson, M.; Smalley, R.; Liu, J. *Nano Lett.* **2004**, *4* (6), 1025–1028. DOI: 10.1021/nl049691d.

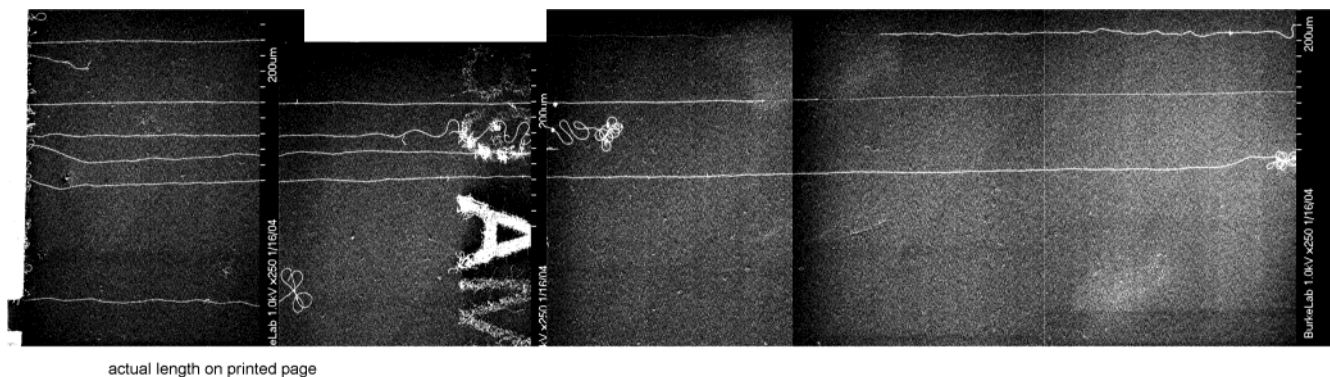


**Figure 1.** Array of 1.5 mm long SWNTs shown in a mosaic of SEM images. Scale bar: 0.5 mm.

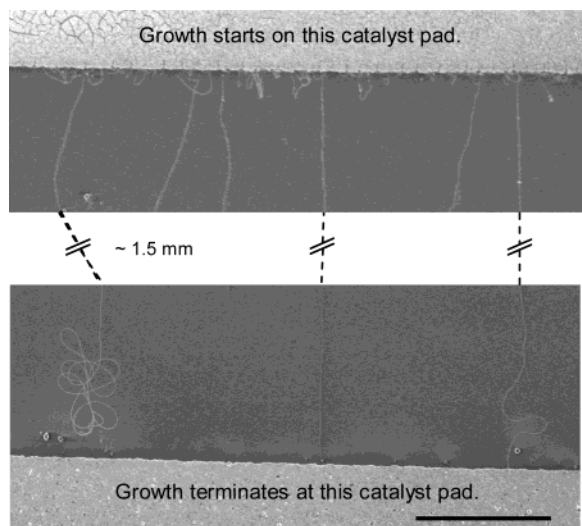


**Figure 2.** High-magnification SEM image of initial and terminal points of long nanotubes shown in Figure 1. Scale bar: 50  $\mu\text{m}$ .

methane (1000 sccm)/ $\text{H}_2$  (200 sccm) mixture was flowed for 15 min to activate the growth. The sample was then allowed to slowly cool in Ar. Post-growth characterization was carried out with SEM (S-4700-2 FESEM, Hitachi, Japan) and AFM (Digital Instruments, Multi-mode).

Before we developed the Au underlayer technique, a series of growth runs with only nanoparticles as catalyst were performed in order to determine the optimum nanoparticle concentration for growth. Five different diluted concentrations (original, 5 $\times$ , 10 $\times$ , 20 $\times$ , and 50 $\times$ ) were prepared and studied in a series of 12 growth runs; each concentration was used in at least two growth runs, except the 50 $\times$  dilution, which was used only once. At high concentration, such as the original and 5 $\times$  dilution, the nanotube growth yield is high. At this high density, the nanotubes tend to overlap and entangle with each other. On the other hand, at low concentration, such as 20 $\times$  and 50 $\times$  dilution, the growth yield is low. The 10 $\times$  diluted nanoparticle catalyst solution afforded the highest number of long nanotubes, although all the nanotubes were less than 100  $\mu\text{m}$  in length for the initial studies without the metal underlayer (see Supporting Information). After optimizing the catalyst concentration, we then turned to studies with a Au metal underlayer to investigate the growth of longer carbon nanotubes.

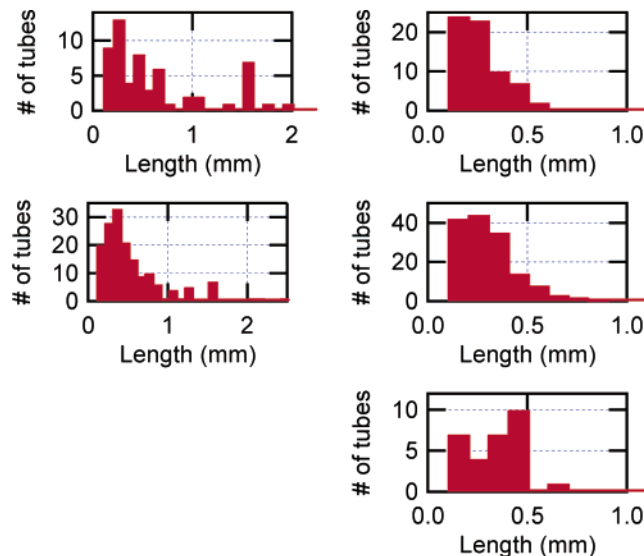


**Figure 3.** Histograms of nanotube lengths from five separate growth runs. Nanotubes less than 0.1 mm in length were not counted in this study.

In Figure 1 we show an SEM image mosaic of a one-dimensional array of ultra-long SWNTs. The growth results indicate an aligned array of six nanotubes with pitch of 50  $\mu\text{m}$  and length of at least 400  $\mu\text{m}$ . Three of the 6 nanotubes were 1.5 mm in length. The growth of the longer nanotubes was terminated only by the presence of a neighboring catalyst site. In Figure 2, we show a higher magnification set of SEM images of the array shown in Figure 1. The catalyst pad initiating the growth shows no outstanding features. From the images, we find three mechanisms for terminating the growth: (1) The nanotube continues to grow straight until it hits the nearest obstacle. (2) The nanotube grows straight over distances on the order of millimeters and then begins to turn with a radius of curvature on the order of 10  $\mu\text{m}$ , terminating in the nearest obstacle. (3) The nanotube grows straight over distances on the order of millimeters and then turns extensively, returning on itself many times, without reaching the nearest obstacle. The third termination mechanism is also visible in Figure 1, for two nanotubes that grew to only 0.7 mm in length. At the moment, the mechanism for a straight nanotube terminating in a loopy section is unknown. Clearly, though, all three mechanisms are related to an obstacle of some sort, which indicates that we have not reached the limits in nanotube length for our growth procedure. In some cases, we find the nanotube growth



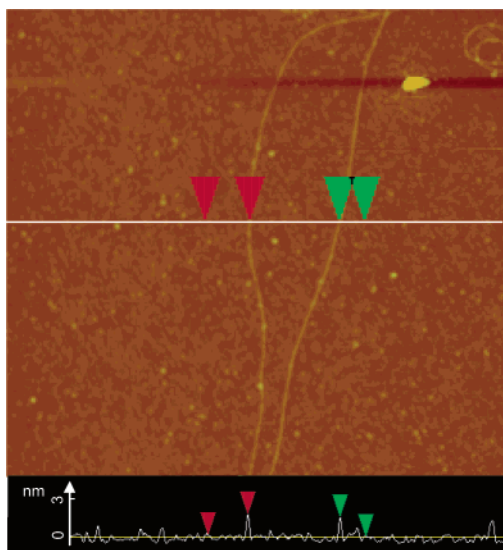


**Figure 4.** AFM image of nanotubes, showing a height of 1.7 and 1.6 nm. Image area is  $1 \times 1 \mu\text{m}$ .

terminates before it reaches an obstacle. For these nanotubes, we believe the growth initiated sometime after the beginning of the growth run and then terminated when the methane flow was halted. However, we cannot rule out the possibility that an alternative, unknown mechanism exists to terminate nanotube growth.

To quantify the length of the nanotubes, we have carefully analyzed the results of five separate growth runs, corresponding to three separate catalyst depositions. We plot in Figure 3 five histograms of the number of nanotubes grown vs length. For each run, we carefully measured the length of all the nanotubes grown from 1/3 of the 18 catalyst pads on the chip, each pad being  $1 \times 2 \text{ mm}$  in size. In five other growth runs we performed, although we did not perform as detailed an analysis, we found similar results. Thus, our results are reproducible from growth run to growth run (for 10 runs total) and from catalyst deposition to catalyst deposition.

In Figure 4, we plot an AFM image of nanotubes synthesized with our growth procedure, indicating a height of 1.6 and 1.7 nm. AFM images of other nanotubes synthesized with the same procedure yield diameters ranging from 1.4 to 1.9 nm. TEM imaging (see Supporting Information) indicates that our long nanotubes are individual single-walled nanotubes and not bundles. Additional TEM images (not shown) indicate that our shorter nanotubes ( $< 10 \mu\text{m}$ ) are single-walled with bundles occasionally occurring. Thus, we find that the long nanotubes are indeed isolated, individual SWNTs.

The ability to grow these ultra-long, straight nanotubes is due to two key factors: First, we have designed a special gas injector to efficiently mix the gases before flow and minimize the turbulence (see Supporting Information). This allows the nanotubes to grow long distances in a single direction parallel to the gas flow. Second, the Au underlayer supports the nanoparticle

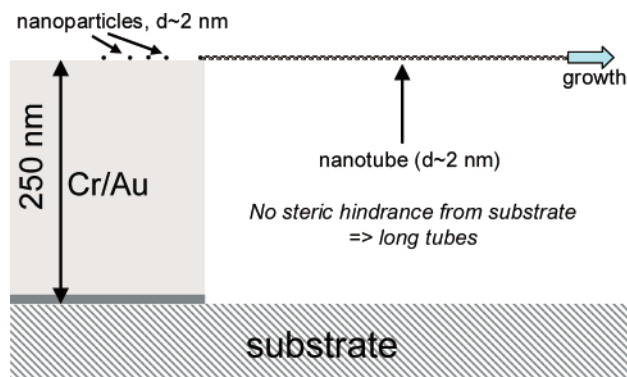


**Figure 5.** To scale schematic drawing of nanotube growth from elevated catalyst sites.

catalysts well above the substrate,  $\sim 100$  times larger than the nanotube and nanoparticle diameter. This allows the nanotubes to grow without interference from the substrate over long distances. In dozens of control experiments with no metal underlayer (see Supporting Information), we found no carbon nanotubes longer than  $100 \mu\text{m}$  in length. We postulate that, during growth, the nanotubes are freely suspended and that, after the growth, the nanotubes gently settle to the substrate and become van der Waals-bound there. This is indicated schematically in Figure 5. This is unique to our growth procedure. Evidence for this is given in the Supporting Information, where an SEM image shows the beginning of a  $0.65 \text{ mm}$  long nanotube. The image shows the nanotube is freely suspended between the catalyst and the substrate, indicating that growth initiated from a nanoparticle that was well above the substrate. Although we know the as-grown nanotubes are parallel to the gas flow direction, for the studies presented here we do not know if the nanotubes grew in the *upstream* or *downstream* direction; this will be addressed in future work.

In conclusion, we have demonstrated the growth of 1d arrays of millimeter long SWNTs using a single-furnace, methane/ $\text{H}_2$  recipe. In the future it should be possible to grow 2d arrays by rotating the wafer and carrying out a second growth run. By engineering the nanotube pitch through careful catalyst preparation, ultra-dense electrical circuitry could be fabricated.

**Acknowledgment.** This work was supported by the Army Research Office (Award DAAD19-02-1-0387), the Office of the Naval Research (Award N00014-02-1-0456), and DARPA (Award N66001-03-1-8914). We thank Jake Hess of the INRF for assistance with the construction and design of the CVD system, Dr. Wen-An Chiou of the Materials Characterization Center for assistance with TEM imaging, and Dr. Q. Xu of the INRF.

**Supporting Information Available:** Additional figures (PDF). This material is available free of charge via the Internet at <http://pubs.acs.org>.

CM049503K